

Nonlinear effects of current on transport in manganite films

Akilan Palanisami,¹ M. B. Weissman,¹ and N. D. Mathur²

¹*Department of Physics, University of Illinois at Urbana-Champaign, 1110 West Green Street, Urbana, Illinois 61801-3080, USA*

²*Department of Materials Science, University of Cambridge, Cambridge CB2 3QZ, United Kingdom*

(Received 7 April 2004; revised manuscript received 23 December 2004; published 23 March 2005)

In films of $\text{La}_{0.7}\text{Ca}_{0.3}\text{MnO}_3$ at current densities above about 10^4 A/cm^2 a jump in resistance is found when the average sample temperature is just below the temperature of the maximum derivative of Ohmic resistance with respect to temperature. The jump is hysteretic as a function of current, temperature, and magnetic field. The existence of the jump is consistent with simulated effects of nonuniform Joule heating. Local thermometers based on noise features provide further evidence for the nonuniform heating. However, detailed comparison of the simulated Joule effects and the data show qualitative discrepancies, possibly due to strain-induced mixed-phase texture.

DOI: 10.1103/PhysRevB.71.094419

PACS number(s): 75.47.Lx, 75.80.+q, 72.60.+g, 72.70.+m

INTRODUCTION

The perovskite manganites have received heavy scrutiny as a result of their many unconventional behaviors.^{1,2} Large nonlinear transport effects of both signs are among the more intriguing reported effects.³⁻¹³ Many of these nonlinear effects have often been attributed to depinning transitions or to melting of charge order (CO). Although Joule heating has usually been considered as an obvious contributor to nonlinear transport, it has typically been rejected as a major contributor to the interesting effects in manganites.

In this paper we examine the effects of high current densities in $\text{La}_{0.7}\text{Ca}_{0.3}\text{MnO}_3$ (LCMO) films. These effects include a weakly hysteretic first-order transition. Simulations based on realistic patterns of resistivity (ρ) vs temperature (T) show that this effect can be semiquantitatively accounted for by spatially varying Joule heating. We present noise measurements providing local thermometers confirming the spatially inhomogeneous heating. However, we find major discrepancies between the simulations and the data. We attribute these to effects of a mixed-phase texture maintained by strain interactions. Such texture would create hot spots, which help trigger the transition at lower temperature than it would otherwise occur, while the underlying interactions inhibit runaway to a uniformly insulating state which would otherwise occur.^{14,15}

EXPERIMENTAL METHODS

The samples are made from a low-strain laser-ablated film of optimally doped $\text{La}_{0.7}\text{Ca}_{0.3}\text{MnO}_3$ on a 1-mm-thick substrate of very nearly lattice-matched untwinned (001) NdGaO_3 (NGO), with a magnetic easy axis along the orthorhombic [100] direction. The growth details are outlined in Ref. 16. Atomic force microscopy demonstrated atomic step-flow growth everywhere, indicating a coherently strained film, with some terracing.¹⁷

The film is grown to a 50-nm thickness and subsequently patterned into a 3.7-mm-long bridge with 50- μm -wide wires separated by a 60- μm gap, as shown in Fig. 1. The four-probe bridge pattern allowed for noise measurements with

relatively little sensitivity to contacts or temperature drifts. The total cross-sectional area through which the currents flowed was $5 \times 10^{-8} \text{ cm}^2$, counting the two parallel paths. Gold contact pads at a distance of 150 μm from the bridge were deposited using lift off. Thermal feedback effects are sensitive to the type of bias used. Except where noted, the data shown here were taken with a constant current (I) bias. In the other cases, the use of series resistors with batteries led to a bias intermediate between constant I and constant voltage V .

Since in any thermal feedback model, overall thermal boundary conditions are important, we specify them here. The sample is mounted on a copper cold finger, with the thermometer mounted roughly symmetrically on the other side of the cold finger. T was measured with an Si diode, with reproducibility of about 10 mK, although the absolute accuracy is not that good, so the precision of T 's given below is intended only for internal comparisons.

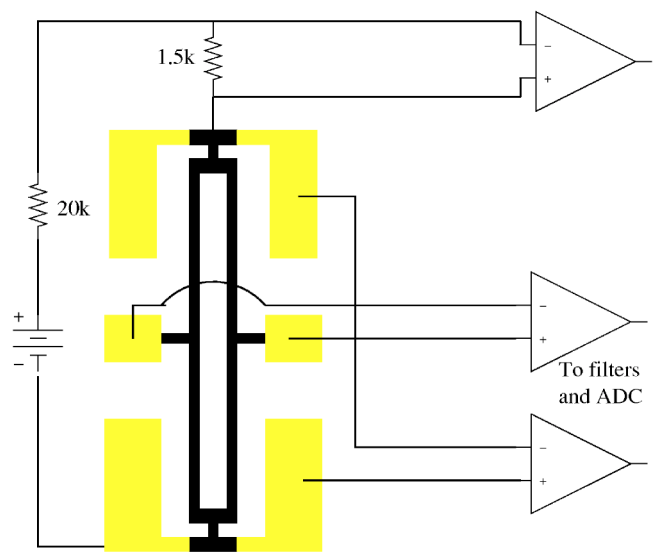


FIG. 1. (Color online) Shows the sample bridge geometry, and schematically indicates the measurement circuit, designed to eliminate any contact noise.

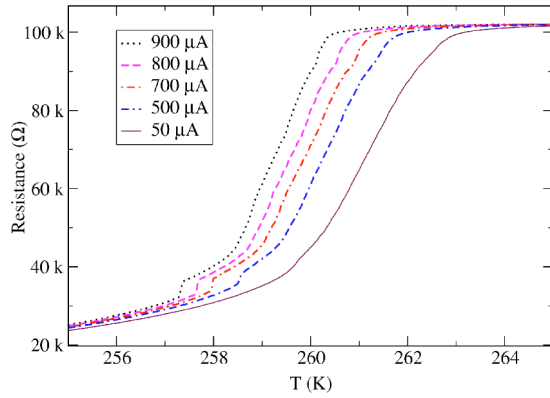


FIG. 2. (Color online) Typical R vs cold finger T taken at different currents on warming.

Connection was made to the gold pads using 0.5-mm gold wire. The leads leading out of the cryostat are wrapped around bobbins several times near the heat exchanger to thermally sink the leads to the heat exchanger. Thermally conducting grease was used to mount the substrate onto a 4-mm-thick copper block. This copper block was bolted tightly on to the cold finger (with thermal grease). A standard thermal shield can was used in the flow through cryostat between the sample region and the outer vacuum can, with no intentionally introduced exchange gas. The chamber was pumped continuously with a sorption pump.

RESULTS AND INITIAL ANALYSIS

Typical R vs T curves, taken at different I , are given in Fig. 2 (T here refers to the cold finger). In this paper we consistently define R to be V/I . The metal-insulator transition (measured at low current) is sharp and little shifted from the bulk transition temperature T_C of approximately 260 K as found previously^{18,19} and as expected from the good lattice match ($<0.1\%$) to the substrate. A narrow peak appears in the low-frequency conductance noise at T_C , similar to previous results,¹⁹ except that we find magnetic-field dependent noise for T at and below the noise peak rather than at and above it. Additional interesting features of the noise are discussed in another work to appear in this journal.

It appears from the shift of the R vs T curves at different currents that I^2R Joule heating is playing a role. The heat dissipation of the sample can be measured directly by examining the R at a constant cold finger temperature as a function of I well above T_C . Here, in the paramagnetic regime, any change in R as a function of I would be expected to be due entirely to Joule heating. We would then expect that plotting R vs the actual sample T , which exceeds the T of the substrate by an average increment $\Delta T = \alpha I^2 R$, would match the low- I $R(T)$. This procedure does in fact work with a value $\alpha = 54$ K/W, not far from expectations from an *a priori* calculation of simple heat conduction, described below. In fact the $R(T)$ taken at different I collapse to a single curve in both the paramagnetic and ferromagnetic regimes, except in a region 258 K $< T < 266$ K, as shown in Fig. 3. Thus differences in thermal properties between the ferromagnetic and

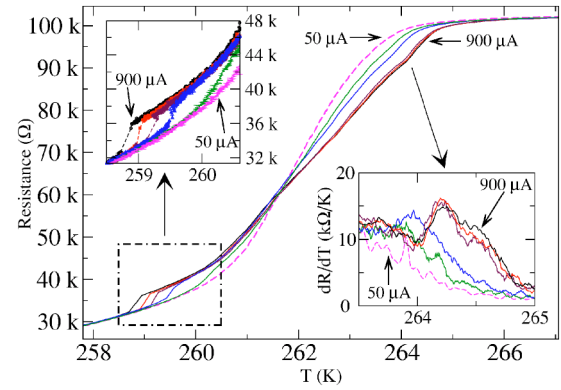


FIG. 3. (Color online) $R(T)$ (with some smoothing) for different I at $H=0$, taken on warming after cooling at $I=0$. The currents are 50, 500, 700, 800, 850, and 900 μA , consecutively as labeled. The curves were corrected for Joule heating via a single temperature-independent coefficient $\alpha = \Delta T/I^2 R$. The curves were repeatable provided the sample had been thermally cycled with current recently. Failure to cycle within 12 h of taking data shifts the $R(T)$ curve ~ 100 mK down in T . The 800, 850, and 900 μA curves overlap in the 260–264 K range. Upper inset: blowup of data, without smoothing, near the jump. The dashed lines guide the eye between data above and below the jump taken at the same current. Lower inset: blowup of derivatives of curves near 264 K. The three curves that nearly overlap are those at 800, 850, and 900 μA .

paramagnetic regimes seem unimportant here, although further complications obviously must be considered in the transition region.

The deviation from collapse occurs in the region of large d^2R/dT^2 , and is of the same sign as d^2R/dT^2 , crossing zero in the vicinity of an inflection point near $T=261.7$ K. Thus the simplest interpretation is that in this regime correction for the spatially averaged ΔT is inadequate, since R is also strongly sensitive to a spread in T . Since the center of the sample will heat substantially more than the edges, this spatial spread in ΔT will be comparable to the average ΔT . The next higher order term in the expansion giving $R(I)$ (at fixed substrate T) will then be a correction proportional to $I^4 d^2R/dT^2$.

There is one striking qualitative deviation from any such finite Taylor expansion fit to the nonlinearity. A jump in R vs T is seen below the T of the maximum dR/dT , with T_j , the temperature of the jump, monotonically decreasing with current I . The jump is hysteretic in T , I , and magnetic field H , as illustrated in Figs. 4 and 5. T_j is at the low- T end of the regime where the first-order Joule correction fails. There is no discontinuity in Ohmic R as a function of true sample T , so a discontinuity in R vs substrate T indicates a positive thermal feedback effect, if Joule heating is the source. Such positive feedback can accentuate the failure of the mean ΔT correction by amplifying some inhomogeneities in the heating.

Near a region of large dR/dT , a small increase in T will increase R substantially. Whether that then reduces or increases the local power dissipation depends on whether that local region is biased close to constant current density or close to constant field, which depends on the geometry of the

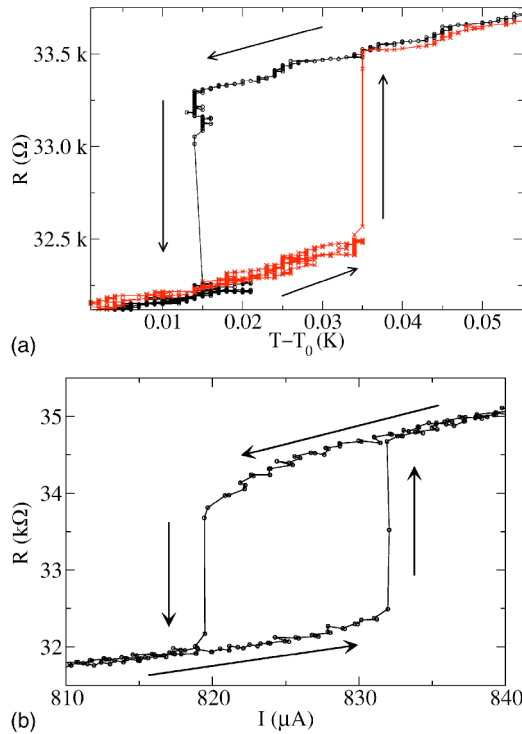


FIG. 4. (Color online) (a) The hysteresis of $R(T)$ is shown at $H=0$. $I=860-880 \mu\text{A}$, set with a battery and series resistor, and thus dependent on R . (b) The hysteresis of $R(I)$ is shown at $H=0$ and $T=260.35$ K.

region as well as whether the sample overall is being operated at constant I or constant V . If the feedback is positive, a thermal runaway can create a discontinuous jump. The lowest-order self-consistent equation for R starting at an Ohmic value R_0 in the presence of Joule heating at fixed I is

$$R = R_0 + \alpha I^2 R \frac{dR}{dT}. \quad (1)$$

No finite positive solution of Eq. (1) for R exists when

$$\alpha I^2 \frac{dR}{dT} \geq 1. \quad (2)$$

Therefore one expects the runaway heating to set in approximately when the left-hand side of Eq. (2) is unity.

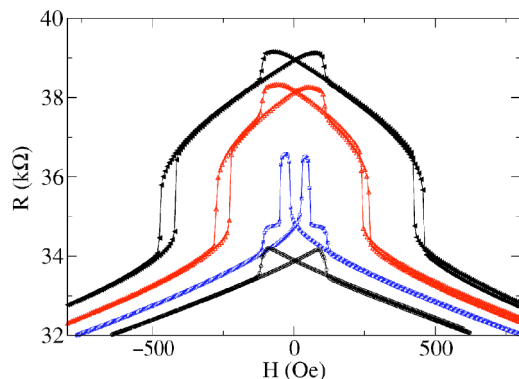


FIG. 5. (Color online) $R(H)$ hysteresis loops at (from bottom) $I=700, 735, 775,$ and $800 \mu\text{A}$ and $T=260.69$ K.

For this sample the lowest current for which condition (2) is met at any T is $I=800 \mu\text{A}$. That current is very close to the minimum actually found to produce a jump, strongly supporting the interpretation that the jumps are artifacts of current heating. However, T_j is well below the T of maximum dR/dT , at which Eq. (2) holds, so that it is essential to consider inhomogeneity of the heating if a thermal explanation is to hold.

Thermal instability should be accompanied by hysteresis. The hysteretic properties can be used to study whether thermal inhomogeneities or magnetic transitions, etc., are more plausible explanations of the jump in R .

The bottom curve in Fig. 5 displays an ordinary R vs H curve at low current. Its hysteretic behavior in R stems from ordinary magnetic hysteresis, with the abrupt drop in R occurring as the sample becomes single domain at the coercive field H_C (e.g., Ref. 20), losing magnetic domain wall resistance.²¹ The properties of this hysteretic jump should be sensitive to any major change in the magnetic domains. As the current is increased, a second hysteretic jump, the same one that appears in the $R(T)$ at $H=0$, first appears near $H=0$ and then smoothly moves out beyond H_C as I is increased. The coercive field of the ordinary hysteretic magnetoresistive jump has almost no dependence on I , regardless of whether it appears on the low or high side of the new jump. The size of the ordinary hysteretic effect is very slightly reduced in the high- I case. There is some effect of current in rounding the curves just before the ordinary coercive field is reached. Thus the hysteretic jump found at high current occurs without any obvious major effects on most of the magnetic domains.

R vs H was checked with H perpendicular to the current, both in and out of the film plane with no qualitative change in the current-induced jump's behavior, other than a smearing of the jump due to field inhomogeneity from demagnetization effects when H was perpendicular to the film. This rules out any global reorientation of the magnetization as an explanation of the jump.

The kinetics of the jump also help limit possible descriptions. The jump occurs rapidly on the time scale of the $R(T)$ measurements, taking less than 1 s. When a small ac (100 Hz) current was superimposed on a dc current well into the nonlinear regime, a spike in second harmonic amplitude was found at the jump, with magnitude close to what would be expected from the dc transport measurements. Thus the anomalous nonlinearity, including the jump, is not due to gradual changes in the sample due to electromigration or other slow effects.

The noise data provide further clear evidence indicating the large thermal inhomogeneity created by the Joule heating and the importance of the feedback in amplifying this effect. Figure 6 shows noise data taken at several bias levels, using the circuit shown in Fig. 1. The large noise peak ordinarily found near T_C serves as a sort of crude local thermometer because it arises when parts of the sample fluctuate between metal and insulator, i.e., are close to their local T_C . At high current, the peak turns into a plateau, with the low- T end coinciding with T_j . The combined noise and resistance data make sense if a fraction of the sample is driven to T near T_C , where it becomes noisy, but most of the sample remains well

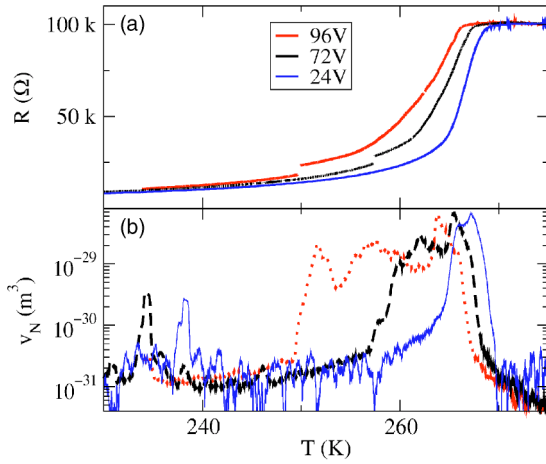


FIG. 6. (Color online) (a) $R(T)$ at three different driving conditions: (24 V at bottom, 72 V, and 96 V at top) in series with a 21.5 k Ω resistor. (b) Normalized noise magnitude (v_N^* in 2= sample volume times voltage noise power from 24–47 Hz divided by squared sample voltage) vs T under those three conditions. The curves with abrupt steps in noise power correspond to those with abrupt steps in R at the same temperatures. The noise data have been smoothed over about 0.5 K. T has not been corrected for Joule heating. R and v_N taken at 12 V were virtually identical to those at 24 V.

below T_C , as seen in R . At high current, as R increases by about 5% right at the jump, the normalized noise magnitude increases by about a factor of 4, although that only represents about 2% of the maximum normalized noise magnitude. For example, in the highest-current trace of Fig. 6, it appears that at T_j some of the sample must have a T increase of about 15 K to reach the noisy regime, although from R one can see that most of the sample does not.

In one case (see Fig. 7) the Boltzmann factor of an individual fluctuating two-state system was tracked vs I and, at low I , vs T . This Boltzmann factor serves as a local ther-

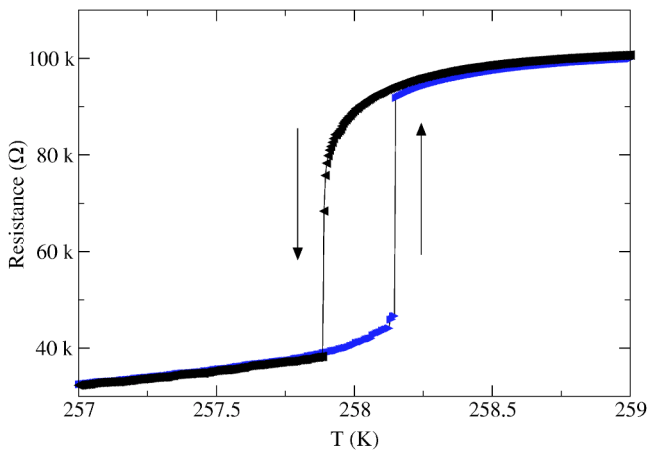


FIG. 7. (Color online) The dependence of the Boltzmann factor for an individual switcher is shown vs actual T (near 200 K) taken at low I and vs T as calculated from Joule heating at different I using the bulk α found at around 260 K. The actual dependence of the Boltzmann factor on current can be fit if the local α is about 1.5 times larger, or roughly 2.0 times larger than the bulk α should be near 200 K.

момeter, allowing the local heating to be tracked. For this particular site, the heating was about 1.5 times as large as would be inferred from the α used to collapse $R(T)$ near 260 K. Since this fluctuator appeared at lower T , and since the thermal conductivity of NGO is a decreasing function of T in this range,²² the heating seen by this fluctuator is actually a factor of 2.0 times as large as would be found if ΔT were uniform.

A closer look at the $R(T)$ curves (corrected for average heating) at high I reveal a second feature, near 264 K, shown in detail in the inset of Fig. 4. This feature is neither discontinuous nor substantially hysteretic. It appears to reach a limiting form at the highest I values.

THERMAL MODELING

The full nonlinear effect of the Joule heating is nontrivial to calculate, because the nonuniform heating leads to nonuniform current density J . Therefore we used numerical calculation to find self-consistent J , ρ , and T spatial distributions for a slab of homogeneous material of roughly the same dimensions as the sample. The simulation first calculates $\mathbf{J}(\mathbf{r})$ from $\rho(\mathbf{r})$, using standard techniques.²³ Next the local power dissipation density $W(\mathbf{r}) = \rho(\mathbf{r})J^2(\mathbf{r})$ is used to find $T(\mathbf{r})$ via the standard three-dimensional (3D) heat diffusion equation, described below. Then the experimental values of $\rho(T)$, obtained from the low- I data, are used to get a new $\rho(\mathbf{r})$. This procedure is iterated until convergence.

To simplify the simulation, several important approximations were made. First, the current distribution is modeled in a two-dimensional geometry. This is justified because the sample is thin enough for thermal differences in the out of plane direction to be insignificant. Second, in calculating $T(\mathbf{r})$, the wire is again treated as a 2D heat source, with all the thermal conduction occurring in the 3D NGO substrate. This approximation is particularly well justified since the thermal conductivity of NGO (Ref. 22) is about eight times larger than that of the thin LCMO (Ref. 24). The T dependence of the thermal conductivity is ignored because of the narrow range of T involved. Finally, the NGO is usually treated as a semi-infinite slab, which is crudely justified because its thickness is comparable to the sample length. The base T is assumed to occur at an infinite distance from the sample. We also tried modeling the finite thickness of the NGO substrate by considering the coldfinger metal as a fixed- T layer at a finite distance from the sample, using the method of images, as for a conducting plane in the electrostatic analog. This modification had only minor effect (about 100 mK shift in T_j) on the calculated nonlinear effects, confirming that the simpler semi-infinite slab model used in the calculations shown would suffice. Introducing constant- T heat sinks to represent the gold contact pads in the simulations had negligible effect.

The 3D heat flow equation then looks exactly like an electrostatics equation with $W(\mathbf{r})$ playing the role of charge density and the $\Delta T(\mathbf{r})$ being similar to the potential, i.e., the heating goes inversely with the distance from the source:

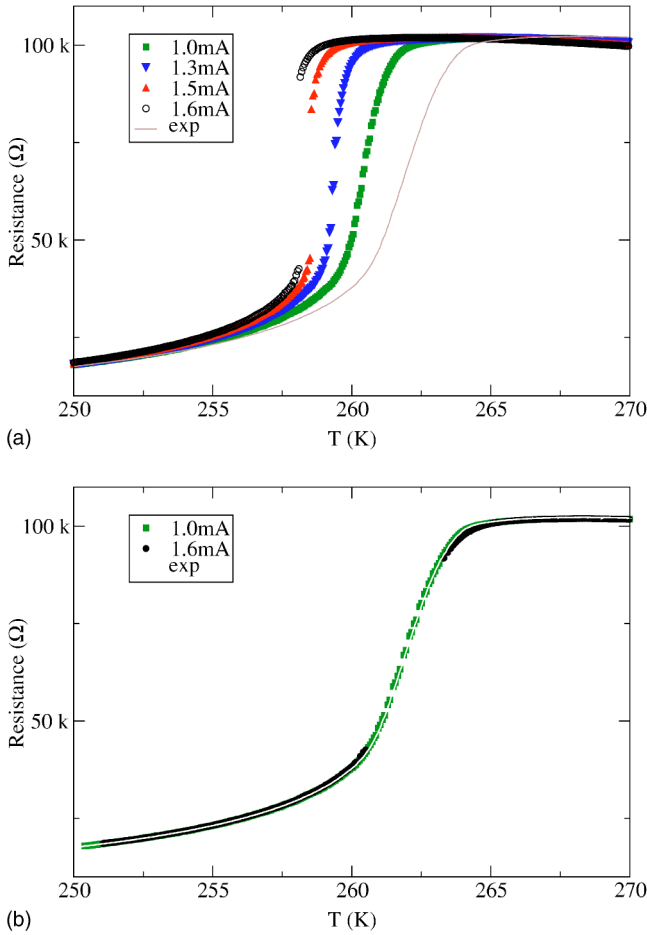


FIG. 8. (Color online) (a) Simulations of R vs substrate T , using the experimental Ohmic $R(T)$ curve, are shown at different simulated currents. (b) Rescaling of the same curves after correcting T for Joule heating via a term proportional to I^2R . The white gap in the midst of the curves is the experimental low- I $R(T)$.

$$\Delta T(\vec{r}) = \left(\frac{1}{2\pi\kappa} \right) \int \frac{W(\vec{r}')}{|\vec{r} - \vec{r}'|} d^2\vec{r}', \quad (3)$$

where κ is the thermal conductivity of the NGO. The diffusion kernel $1/2\pi r$ rather than $1/4\pi r$ arises because the heat diffusion occurs only through half of the 3D environment. In discretizing the integral in Eq. (3) on a square lattice, we include a heating term for each point from its own area increment, for which one cannot divide by a distance of zero but rather can use the analytic integral obtained by treating the $W(r)$ as uniform over a single lattice square.

This simple simulation gives not only Joule heating of about the right magnitude but also an increase in the maximum dR/dT (where T is that of the base, i.e., cold finger), as expected from feedback. A dramatic first-order jump appears, as shown in Fig. 8. Thus a simple Joule heating model, whose only input from the interesting material properties is $R(T)$, reproduces much of the qualitative behavior found.

Nevertheless there are some discrepancies between the simulation results and the experimental data which do not seem likely to be resolvable by minor adjustments to geom-

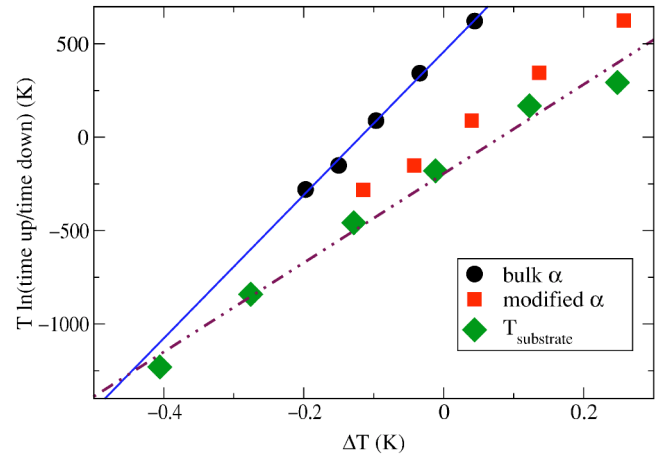


FIG. 9. (Color online) The simulated hysteresis vs T is shown at a simulated current of $1600 \mu\text{A}$.

etry or other such corrections to the simulations. (They are not, for example, affected by inclusion of a thermal conductor plane beneath the finite substrate or by inclusion of contact effects.) There is a small quantitative discrepancy in that the simulations require larger I to trigger the first order jump than found experimentally. The most obvious discrepancy is that the simulation gives too big a jump (as in Fig. 8), with too much hysteresis (Fig. 9), when the average heating is adjusted to be comparable to experimental values. When the experimental current is raised to about 1.3 times the minimum current required to make a jump, the net jump in R is only 4% of the maximum R . The corresponding figure for the simulations exceeds 50%. Furthermore, the value of R on the more insulating side of the transition, just above T_J , is a strongly *increasing* function of I in the simulation, but a weakly *decreasing* function of I in the experiment. In addition, the feature in $R(T)$ experimentally found at high current near the maximum in R is absent in the simulations. The simulations show a near-collapse to a single curve, when corrected for average heating with a fixed coefficient, in contrast to the experimental data which appear to shift from one collapsed curve at low I to another at high I .

A clue as to the origin of the discrepancies is found for the single-fluctuator heating data, which came out to be twice the average heating in the example described above. The simulations show inhomogeneous heating, as in Fig. 10, but the maximum of the heating in the simulations is only 1.09 as large as the average value, since most of the inhomogeneity appears as narrow cool regions along the edge. Thus the enhanced Joule heating of this individual region is further strong evidence of the inhomogeneity of the current density in the metallic regime, previously shown by the large effects of small fluctuators on R .^{14,25,26} The obvious qualitative feature missing from the simulations is this pre-existing gross inhomogeneity of the resistivity, present even at low currents.

This inhomogeneity will lead to hot spots, triggering the resistive jump at lower T and I than would otherwise occur. Since all four arms of the sample nevertheless switch resistive states in a concerted jump, despite inevitable minor irregularities and nonuniformities in lithography and materials,

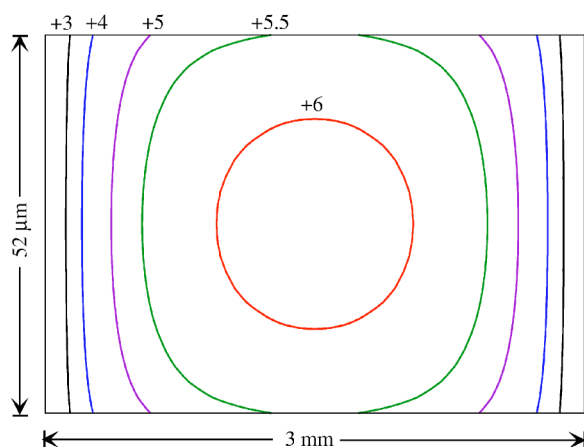


FIG. 10. (Color online) Calculated constant-heating contours are shown for a base T of 258 K and a current of 1600 μA , taken on simulated warming in the hysteretic region. T increase contours are labeled in K. Note the different scales for the current direction (horizontal) and width (vertical), used to enhance visibility.

it is clear that they are linked cooperatively by the long-range heat diffusion.

More importantly, the actual film has some mechanism limiting the runaway conversion to the semiconducting phase, unlike the simulations. The simulations consider only one type of effective interaction between different regions, due to heat diffusion. There appears to be another, anticonoperative, interaction preventing the runaway. Strain interactions due to the constraint imposed by the substrate have been previously suggested to provide just such an anticonoperative effect.¹⁴ They should have a limited range, since the substrate clamping should tend to cut them off on distance scales comparable to the sample thickness.¹⁴ Even in the absence of such constraints, it has been proposed that strain interactions can promote mixed-phase textures in the presence of disorder.¹⁵

The collapse of the experimental higher- I $R(T)$ curves upon correction for average ΔT suggests that there is a well-defined phase texture in the state formed at high I . The reproducible feature found near the upper end of the transition region when the current is high enough to make a jump at the lower end of the region may represent the collapse of that texture as the sample becomes nearly all paramagnetic.

Since all the arms of the sample remain in balance across the resistive jump, such texture must be on a scale much smaller than the sample size. On the other hand, since the ordinary magnetoresistive hysteresis is only moderately affected by the resistive jump, the texture change appears to be on scales at least comparable to those of the magnetic domains and other discrete switching regions, i.e., some thousands of unit cells in volume.^{26–28} Otherwise, the change at T_J would be expected to show up more dramatically in the properties of the magnetic domains which give rise to the ordinary hysteresis.

DISCUSSION

It appears that the hysteretic resistance jump seen in our thin film sample stems from the sharp metal-insulator transi-

tion. Similar phenomena should also be seen in other materials displaying a sharp change in resistance with temperature. For example, hysteretic jumps in the I - V curves of superconducting wires²⁹ may have similar origins. The phenomena found from solving transport models to which the only inputs are realistic $\rho(T)$ functions and realistic thermal flow equations are already quite rich, including hysteresis. Such phenomena arise from sharp features in dR/dT , and thus are likely to be most prominent in the “best” samples, perhaps giving a false impression that other physical effects are required.

It is interesting to consider also the sorts of nonlinear effects which can arise when $dR/dT < 0$, as is found for example in CO manganites.^{3,5–8} Any small cross section of a sample will be under something close to constant current bias, regardless of how the sample overall is biased, because the small cross section is in series with longer sections. When $dR/dT < 0$, the feedback effects would promote nonuniformity across the sample, since a region of high T would pull in more current and heat further. This effect should be considered as a possible cause or contributor to the formation of filamentary conduction under strong current bias.

It is difficult to go through prior papers on nonlinear effects in manganites to determine what role is played by Joule heating, in part because data on the thermal environment is often not described in detail. Certainly many prior works cite effects, such as long-term memory persisting after current is switched off,^{6,10} which cannot possibly be explained by Joule heating. In other cases^{4,9} derivatives of resistivity with respect to base temperature seem inconsistent with simple Joule explanations. In one case¹¹ anisotropy together with characteristic tunneling nonlinearities indicate non-Joule nonlinearities. Sometimes the combination of the form of the nonlinearity and the associated transport noise suggests a depinning effect.³ Often, however, it is unclear from the published data whether Joule effects, especially allowing for nonuniformity, might play a significant role in nonlinearities.

While material-specific inputs other than $\rho(T)$ may indeed be necessary for a detailed description, e.g., to capture the distinction between our measured and simulated hysteresis curves, they are not trivial to identify. Identifying really interesting physics (e.g., depinning phenomena) may be harder than has been generally recognized. In our manganite sample, the interesting physics—the phase texture and the role of strain in making the phase change in neighboring regions anticonoperative^{14,15}—appears to limit the dramatic nonlinear effects which would be present in a simpler system.

ACKNOWLEDGMENTS

This work was funded by NSF Grant No. DMR 02-40644 and by the UK EPSRC and Royal Society, and used facilities of the Center for Microanalysis of Materials, University of Illinois, which is partially supported by the U.S. Department of Energy under Grant No. DEFG02-91-ER45439. We thank M. B. Salamon and Ch. Simon for discussing their unpublished data. We are especially grateful to P. Monod and L. Granja for crucial advice steering us away from a mistaken interpretation.

- ¹A. P. Ramirez, *J. Phys.: Condens. Matter* **9**, 8171 (1997).
- ²E. Dagotto, T. Hotta, and A. Moreo, *Phys. Rep.* **344**, 1 (2001).
- ³A. Guha, A. Ghosh, A. K. Raychaudhuri, S. Parashar, A. R. Raju, and C. N. R. Rao, *Appl. Phys. Lett.* **75**, 3381 (1999).
- ⁴H. Oshima, K. Miyano, Y. Konishi, M. Kawasaki, and Y. Tokura, *Appl. Phys. Lett.* **75**, 1473 (1999).
- ⁵J. Stankiewicz, J. Sesé, J. García, J. Blasco, and C. Rillo, *Phys. Rev. B* **61**, 11 236 (2000).
- ⁶S. Srivastava, N. K. Pandey, P. Padhan, and R. C. Budhani, *Phys. Rev. B* **62**, 13 868 (2000).
- ⁷A. Guha, A. K. Raychaudhuri, A. R. Raju, and C. N. R. Rao, *Phys. Rev. B* **62**, 5320 (2000).
- ⁸A. Guha, N. Khare, A. K. Raychaudhuri, and C. N. R. Rao, *Phys. Rev. B* **62**, R11 941 (2000).
- ⁹C. N. R. Rao, A. R. Raju, V. Ponnambalam, S. Parashar, and N. Kumar, *Phys. Rev. B* **61**, 594 (2000).
- ¹⁰Y. Yuzhelevski, V. Markovich, V. Dikovskiy, E. Rozenberg, G. Gorodetsky, G. Jung, D. A. Shulyatev, and Y. M. Mukovskii, *Phys. Rev. B* **64**, 224428 (2001).
- ¹¹J. Klein, J. B. Philipp, G. Carbone, A. Vigliante, L. Alff, and R. Gross, *Phys. Rev. B* **66**, 052414 (2002).
- ¹²S. Mercone, A. Wahl, C. Simon, and C. Martin, *Phys. Rev. B* **65**, 214428 (2002).
- ¹³L. Sudheendra and C. N. R. Rao, *J. Appl. Phys.* **94**, 2767 (2003).
- ¹⁴R. D. Merithew, M. B. Weissman, F. M. Hess, P. Spradling, E. R. Nowak, J. O'Donnell, J. N. Eckstein, Y. Tokura, and Y. Tomioka, *Phys. Rev. Lett.* **84**, 3442 (2000).
- ¹⁵K. H. Ahn, T. Lookman, and A. R. Bishop, *Nature (London)* **428**, 401 (2004).
- ¹⁶M. H. Jo, N. D. Mathur, N. K. Todd, and M. G. Blamire, *Phys. Rev. B* **61**, R14 905 (2000).
- ¹⁷M. Paranjape, A. K. Raychaudhuri, N. D. Mathur, and M. G. Blamire, *Phys. Rev. B* **67**, 214415 (2003).
- ¹⁸N. D. Mathur, M.-H. Jo, J. E. Evetts, and M. G. Blamire, *J. Appl. Phys.* **89**, 3388 (2001).
- ¹⁹P. Reutler, A. Bensaid, F. Herbstritt, C. Höfener, A. Marx, and R. Gross, *Phys. Rev. B* **62**, 11 619 (2000).
- ²⁰J. O'Donnell, M. S. Rzchowski, J. N. Eckstein, and I. Bozovic, *Appl. Phys. Lett.* **72**, 1775 (1998).
- ²¹N. D. Mathur, P. B. Littlewood, N. K. Todd, S. P. Isaac, B.-S. Teo, D.-J. Kang, E. J. Tarte, Z. H. Barber, J. E. Evetts, and M. G. Blamire, *J. Appl. Phys.* **86**, 6287 (1999).
- ²²W. Schnelle, *J. Phys. D* **34**, 846 (2001).
- ²³S. Kirkpatrick, *Rev. Mod. Phys.* **45**, 574 (1973).
- ²⁴D. W. Visser, A. P. Ramirez, and M. A. Subramanian, *Phys. Rev. Lett.* **78**, 3947 (1997).
- ²⁵H. T. Hardner, M. B. Weissman, M. Jaime, R. E. Treece, P. C. Dorsey, J. S. Horwitz, and D. B. Chrisey, *J. Appl. Phys.* **81**, 272 (1997).
- ²⁶A. Palanisami, R. D. Merithew, M. B. Weissman, and J. N. Eckstein, *Phys. Rev. B* **64**, 132406 (2001).
- ²⁷R. D. Merithew, Ph.D. thesis University of Illinois, 2000.
- ²⁸B. Raquet, A. Anane, S. Wirth, P. Xiong, and S. von Molnar, *Phys. Rev. Lett.* **84**, 4485 (2000).
- ²⁹J. A. Bonetti, D. J. V. Harlingen, and M. B. Weissman, *Physica C* **388-389**, 343 (2003).